Astron. Astrophys. 334, 845–856 (1998)

ASTRONOMY AND ASTROPHYSICS

The relationship between the WR classification and stellar models

II. The WN stars without hydrogen

Lindsey F. Smith[1] **and A. Maeder**[2]

[1] University of Sydney, Chatterton Astronomy Department, Sydney, NSW 2006, Australia
[2] Observatoire de Genève, CH-1290 Sauverny, Switzerland

Received 5 May 1997 / 30 January 1998

Abstract. We consider the relationships between the classification parameters of WN stars in the new 3-dimensional classification of Smith et al. (1996) and the corresponding and related parameters that define stellar atmosphere models. Specifically, we consider: FWHM of HeII 4686 vs. v_∞; hydrogen content by direct inspection vs. hydrogen content by modelling and vs. colour $(b\text{-}v)_0$; ionisation subclass and M_v vs. effective temperature. From these data we argue that the WN b and *only* the WN b stars (i.e. stars with EW 5411 $>$ 40 Å or FWHM 4686 $>$ 30 Å) are entirely free of hydrogen.

For the WN b stars, we consider the relationships of EW 5411 and FWHM 4686 to the derived temperature T_*; the mass loss rate; and the surface mass flux. It appears that, to first approximation, the stars are a one-parameter family and the spectral classification criteria are sufficient to give an indication of the intrinsic colour, absolute magnitude (not very accurately), effective temperature T_* and terminal velocity.

Theoretical models suggest that the critical parameter defining most of the properties of a WN b star is its present mass. However, the behaviour of FWHM 4686 suggests the presence of a second parameter that affects the mass loss rate and terminal velocity of the wind. We suggest that the second parameter may be either (or a combination of) the internal mean molecular weight or the rotation rate of the star.

We further compare the relationships predicted by evolutionary models with those found for observed stars (using atmosphere models), highlighting the present difficulties in these comparisons.

Key words: stars: evolution; Wolf-Rayet; abundances

1. Introduction

In a previous paper on WC stars (Smith & Maeder 1991, Paper I), we have shown that the abundance ratio (C+O)/He is the primary parameter defining the classification of WC subtypes. On this basis it was possible to explain the luminosity-subclass relationship and the number statistics of WC subclasses in galaxies and regions of different metallicities.

Recently a three-dimensional spectroscopic classification for WN stars has been proposed by Smith et al. (1996, henceforward SSM96). Our aim is to determine the relationship between the three parameters of this classification and the theoretical quantities that describe stellar models. While stellar models lead to the expectation that a WN star is fully defined by its mass and remaining hydrogen content, the reality appears rather more complicated and we shall, in this paper, discuss in detail only the WN stars with no remaining hydrogen. Such stars are essentially helium-stars, with a few thousandths of a percent of nitrogen and a core containing a mixture of helium, carbon and oxygen. The models suggest that such stars form an essentially one-parameter family and that the present stellar mass is the key parameter (cf. Maeder 1983; Langer 1989a; Schaerer & Maeder 1992).

Sect. 2 compares the spectroscopic classification parameters with corresponding model parameters. Sect. 3 considers the effect of hydrogen content on T_* and M_v and identifies the WN b stars as the group that are entirely hydrogen free. Sect. 4 considers the relationships between EW 5411, FWHM 4686 and T_*. We discuss the degree to which the WN b stars appear to be a one-parameter family and the apparent need for a second parameter. Sect. 5 compares atmosphere and evolution models. Sect. 6 considers possible "second parameters" that might affect the terminal velocity of the wind. Sect. 7 presents our conclusions.

2. The classification parameters

The new classification by SSM96 uses:

- Ionisation subclasses: WN2-8 with ionisation decreasing to increasing subclass number. These were created by Beals (1938), modified by Smith (1968a) and extended to WN11 by Crowther et al. (1995a). The new system defines WN2-8 mostly by the ratio of HeII 5411/HeI 5875 (peak line/continuum ratios, not EW).
- A broad-narrow division; b for broad or nothing for "not-b". This distinction was originated by Hiltner & Schild (1966) and reintroduced by Schmutz et al. (1989). Hamann et al. (1993, henceforward HKW93) use the letters s and w for strong and weak line stars. "b" is defined in the new system

by the EW of HeII 5411 $>$ 40 Å or the FWHM of HeII 4686 $>$ 30Å.

- Hydrogen subclasses, with the presence of hydrogen detected by a "bumpy" Pickering series: h for detected; (h) for marginal; o for not detected. The correlation of this parameter with many others was highlighted by Hamann et al. (1995, henceforward HKW95). ha indicates the presence of absorption lines originating from the WR star.

We first examine the numerical relationships between the classification parameters, their stellar model equivalents and other closely related quantities.

2.1. FWHM 4686 vs. other measures of the terminal velocity v_∞

Fig. 1 shows FWHM 4686 (from SSM96) vs. other measures of the terminal velocity v_∞. Values from Hamann et al. (1995) were estimated from the width of helium lines in the visible. Values from Eenens & Williams (1994) were derived by fitting to the P Cygni profiles of HeI 1.083 μ and 2.058 μ. Values from Prinja et al. (1990) were derived from the short wavelength edge of the saturated CIV 1548 violet edge. Correlation is good with the two determinations that depend on helium lines but less good with the UV values. The solid line in the diagram is the regression line fitted to the Eenens & Williams data (filled points) and represents the data with a standard deviation of 174 km/s. It is:

$$(\tfrac{v}{100\,km/s}) = 0.28\,(\tfrac{FWHM\,4686}{\text{Å}}) + 7.7$$

The regression line fitted to the HKW data is slightly steeper (dot-dash line, slope 0.32, intercept 6.4), and the line to the Prinja data (ignoring the outliers discussed below) is slightly flatter (dotted line, slope 0.24, intercept 9.8). The differences are only marginally significant.

The stars with derived terminal velocities well above the line in Fig. 1 (both the HKW and Prinja et al. data sets) are identified in Fig. 1 by their numbers in the Sixth Catalogue (van der Hucht et al. 1981). They are distinguished from the rest of the stars in the diagram by having relatively weak lines. WR 2 (WN 2b) and WR 3 and 46 (WN3b) have lines between 2 and 9 times weaker than WN 3 and 4 stars of comparable line width (see SSM96). WR 22, 24, 25 and 89 are ha stars. WR 128 is the only known WN 4h star and has the weakest lines of any star in this ionisation subclass. The apparent implication is that these stars, with the weakest lines, have a different wind velocity structure from the majority of WN stars.

2.2. Hydrogen abundance

Fig. 2 shows the plot of H^+/He^{++} (by number) from visual inspection of the Pickering series vs. H/He (by number) from the model fits. For WN 8 stars, H^+/He^{++} overestimates H/He by about a factor of 2, reflecting the presence of significant amounts of He^+. For WN7 stars, H^+/He^{++} is a good estimator

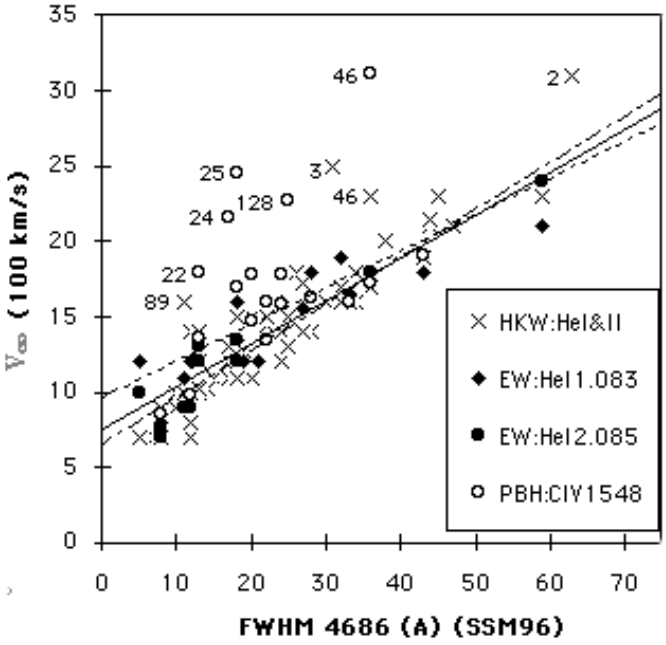

Fig. 1. Relation between FWHM 4686 (Smith et al. 1996) and the terminal velocities derived by Hamann et al. (1995, crosses and dot-dash line), Prinja et al. (1990, open circles and dashed line) and Eenens & Williams (1994, filled symbols and solid line).

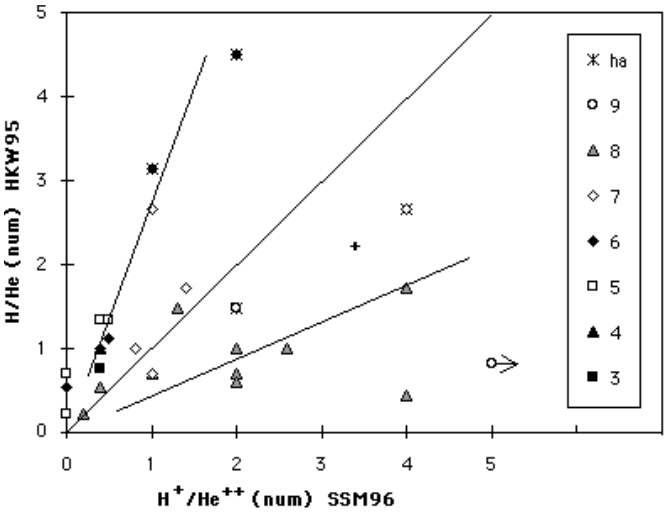

Fig. 2. Relationship between the H^+/He^{++} ratio (by number) from SSM96 and the H/He ratio from HKW95. Notice the dependence on the ionisation subclass, as discussed in the text.

of H/He. For WN 3-6 stars, H^+/He^{++} underestimates H/He by about a factor of 2, possibly due to blending of NIII with the HeII when the lines become broad.

The sequence of decreasing hydrogen contribution to the spectrum is indicated by the hydrogen subclasses: ha, h, (h) and o. Detection by visual inspection becomes unreliable below H^+/He^{++} = 0.5, the boundary between h and (h). There are only two stars with either H^+/He^{++} or H/He below 0.45 (X_H = 0.1, by mass), indicating that the two methods suffer a detection limit at about the same value. The number of stars in any range

of H/He clearly increases to lower values, so there must be a significant number of stars with H/He < 0.5 where detection is difficult.

We note the detection by HKW95 of hydrogen in WR 136, 138 and 157, stars for which hydrogen is not detected from visual inspection of the spectra. We do not change the classification of the stars in what follows, adopting the policy that the spectral classification should reflect only what is available from visual inspection of the spectra. By this policy, the controversial (h) on the classification of WR 136 is inappropriate since the Pickering series for this star is, to visual inspection, completely smooth.

Fig. 3a shows the (b-v)$_0$ derived by HKW95 from model fits to spectra of galactic WR stars vs. $\log T_*$ with the symbols indicating the broad, b, and hydrogen subclasses: ha, h and o; (h) is included with h. We notice that there is a clear relationship between (b-v)$_0$ and the broad, b, and hydrogen subclasses of WN stars; the b-stars separate strikingly from the narrow-line stars and the hydrogen subclasses also separate.[1]

Schmutz (private communication) has pointed out that, without an extended atmosphere, all WN stars are hot enough to have (B-V)$_0$ = -0.3 and that the colour derived from a model depends directly on the extension of the atmosphere, i.e. optical thickness of the wind. Hence, the extreme values in Fig. 3a are not surprising: models that fit b stars have optically thick extended atmospheres and are redder; models that fit ha stars have no extension and are at the blue limit. However, Fig. 3a suggests that the h subclass alone is sufficient to predict (b-v)$_0$. If true, this could provide a simple method for deriving the colour excess of any individual star. But is it true for the real stars as distinct from models fitted to the helium lines of those stars?

For galactic WN stars, the only independent E_{b-v} values are those of Lundström & Stenholm (1984). Schmutz & Vacca (1991) have shown that, the E_{b-v} derived using models agree well, indicating that the models also predict the correct continuum shape - at least for that subset.

For LMC WN stars, Fig. 3b shows observed colours that have been dereddened by nulling the 2150 Å feature (Morris et al. 1993, Vacca & Torres-Dodgen 1990). Scatter in the data is much larger than in Fig. 3a, but the trend is similar. Average values for the galactic models and for the LMC reddened stars are given in Table 1.

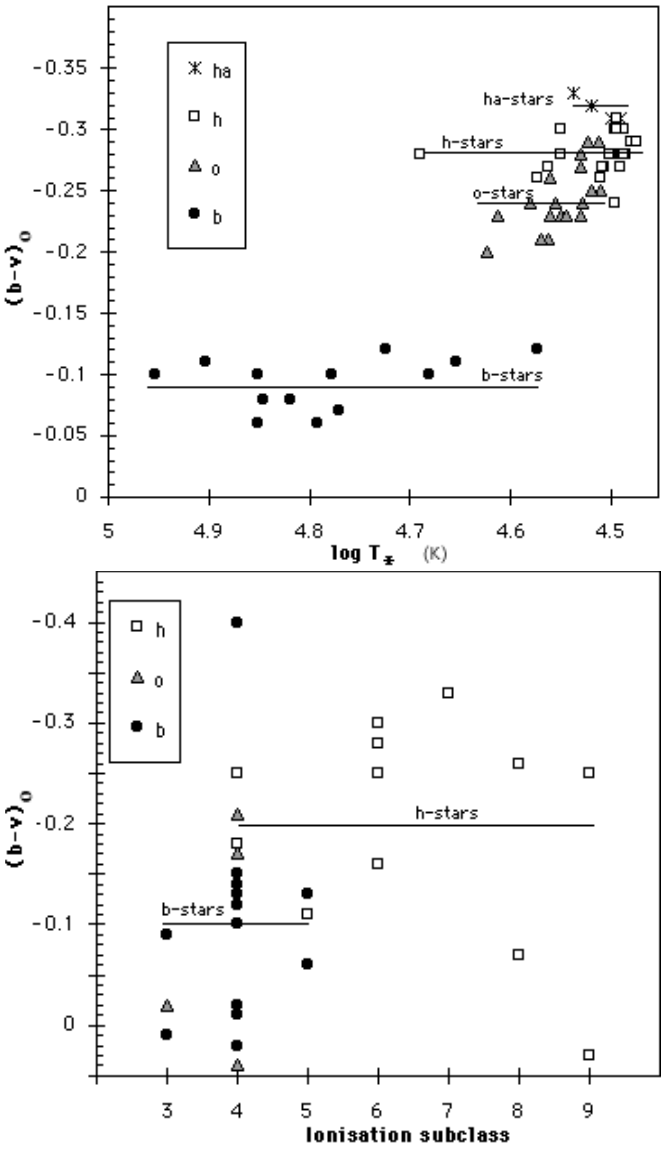

Fig. 3a and b. The intrinsic colour (b-v)$_0$ of WN stars. Different symbols indicate the broad, b, and hydrogen subclasses: ha, h and o. **a** Galactic star colours are from HKW95, derived from model fits to the helium lines vs. $\log T_*$. **b** LMC star colours are from direct observation (Morris et al. 1993, and Vacca & Torres-Dodgen 1990) dereddened by nulling the 2150 Å feature. They are plotted vs. ionisation subclass.

It is not clear whether the scatter in the LMC data (Fig. 3b) and the redder colours of the LMC o and h stars is due to the effect of crowding on the LMC photometric data (cf. Schmutz & Vacca 1991), or whether there is more than one parameter needed to define the atmospheric extent and intrinsic colour of a WN star.

[1] WR 3 and 46 (WN3b) are not plotted in Fig. 3a and are excluded from further discussion. The models for these stars have optically thin winds and blue colours, a result that follows from the weakness of the lines. However, line weakness may be due to the presence of companions. They are both spectroscopic binaries and WR 3 is also a spectrum binary (see SSM 96). On the assumption that the WN stars conform to the otherwise tight correlation of line strength and width, SSM96 estimate the O/WR visual continuum ratios as 6 and 3 respectively. If true, this would invalidate the models of HKW95 which do not allow for the contribution of a companion to the continuum. Their outlier position in Fig. 1 lends some credence to the possibility that the line weakness is intrinsic to the stars, in which case they depart dramatically from the otherwise universal correlation of line strength and width and are very different from the WN3b stars in the LMC which conform to that correlation.

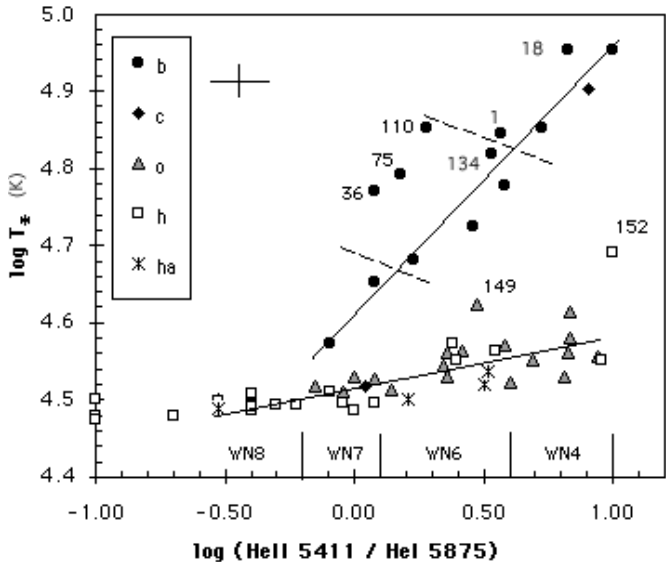

Fig. 4. Relationship between the primary ionisation subclass parameter log HeII 5411/HeI 5875 and log T_*, the effective temperature at τ = 10 derived by HKW (93 and 95) from model fits to the helium lines. The symbols indicate the broad, b, and hydrogen subclasses: ha, h and o. The error bars are one σ and are discussed in the text.

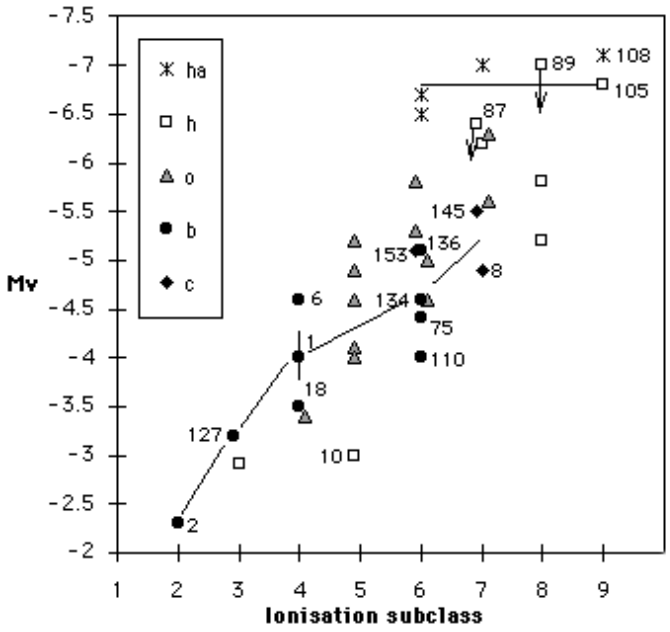

Fig. 5. Relationship between M_v and ionisation subclass with different symbols indicating the broad, b, and hydrogen subclasses: ha, h and o. The hydrogen contribution to the spectrum decreases along the sequence ha-h-o. The label c is used for the WN/C stars. The uncertainty of ± 0.25 mag characteristic of cluster distance modulae is shown on WR 1 (WN 4b). Binaries are plotted with a leftwards displacements of 0.1 subclass and have higher uncertainties. (o-stars are displaced rightwards to avoid overlap of points.) WR 87 (WN 7h+abs) and WR 89 (WN 8h+abs) are marked with downward arrows, indicating the possible contribution by a companion.

Table 1. Average $(b\text{-}v)_0$ of WN stars in the Galaxy and the LMC

Subclass	Galaxy (1)			LMC (2)		
	Average	n	S.D.	Average	n	S.D.
WN b	-0.09	14	0.02	-0.10	15	0.10
WN o	-0.24	18	0.03	-0.09	4	0.12
WN h	-0.28	23	0.02	-0.20	12	0.11
WN ha	-0.32	4	0.01	...		

(1) From model fits by HKW
(2) From direct observations (Morris et al. 1993 Vacca & Torres-Dodgen 1990) dereddened by nulling the 2150 feature.

2.3. Ionisation subclass

Fig. 4 shows the ionisation subclass parameter HeII 5411/HeI 5875 vs. log T_*, the effective temperature at optical depth τ = 10 (HKW95) from model fits to the helium lines. The symbols indicate the broad, b, and hydrogen subclasses: ha, h and o. The label c is used for the WN/C stars. The ionisation subclass boundaries are indicated on the HeII/I axis. The error bar on log T_* of ± 0.1 dex is the standard deviation of differences between the determinations by HKW95 and by Crowther et al. (1995a), both using pure helium atmospheres. The error bar on log HeII/I of ± 0.11 is the standard deviation of differences between various determinations, as tabulated by SSM96 (Table 9).

HKW95 have emphasised that the previously defined ionisation subclasses are not well separated by T_*. With ionisation subclasses in the new system defined primarily by the HeII/I ratio, the same criteria as used to define T_*, we might expect some improvement. The clear separation of b-stars from narrow-weak line stars discovered by Schmutz et al. (1989) and demonstrated further by HKW93 is obvious. Within each group, there is a correlation between the HeII/I ratio and T_*. (A possible reason for the difference in log T_* at the same log HeII/I will be suggested in Sect. 4.2.)

For the b-stars, the ionisation subclasses are approximately separated by T_* boundaries indicating that, in this group, T_* is probably the primary parameter controlling the ionisation subclass. However, the scatter is considerable and three stars in particular, WR 36, 75 and 110, lie at low values of log HeII/I for their values of log T_*. Clean separation of the ionisation subclasses requires sloped (dashed) lines. While this could be an artefact of the observational scatter, the possible relevance of a second parameter is addressed in Sects. 4.2 and 6.

For the narrow-weak line stars, the scatter around a mean line is less than two standard deviations in log T_* (as derived above), however the small difference in average log T_* between the ionisation subclasses suggests that, for this group, another parameter may be dominant. There appears to be no significant separation of the hydrogen subclasses. (A plot against the effective temperature at τ = 2/3 from HKW95, is very similar but with less separation between the two groups, less scatter in the b-stars but more in the narrow-line stars.)

We note the presence of two stars in the gap between the two groups: WR 149, which is included by HKW95 as an s-star but which fails the b-star criteria, and the WN3(h) star WR 152.

Fig. 5 shows ionisation subclass vs. M_v, with different symbols indicating the broad, b, and hydrogen subclasses: ha, h and o. The M_v data are (with exceptions listed in Table 2) from HKW (93 and 95) who dereddened the stars using the $(b\text{-}v)_0$ values from the models. For binaries, we have corrected the M_v using the methods of line diminution of the Balmer and HeI lines of the O stars (Smith & Maeder, 1989) and of the HeII 5411 emission line of the WR star using the calibration from SSM96. New or revised distance modulae are used for WR 6, 78, 108, 78, 157 and 138. All revised data are given in Table 2. (WR 46 is included in Table 2 but not plotted because the values are too uncertain.)

The new elements in this often-produced diagram (which looks rather different from the recent version by HKW95) are: revised ionisation classifications; improved values for WN stars in binaries and inclusion of information about the amount of hydrogen. We note the following points:

- The overlap in M_v of adjacent ionisation subclasses is considerable and the spread within a subclass appears to be larger than the uncertainties.
- The WN 6-8 stars in particular spread over several magnitudes; however, the brighter stars are spectroscopically distinguished as "ha" stars.
- The WN5 stars (in this diagram) are all binaries and there are no b-stars. While the sample is only those stars with known M_v, the dominance of binaries and low proportion (or lack of) b-stars is a general properly of WN5 (see SSM96).
- For WN 6-9 stars, the hydrogen richer stars are brighter. Brightness decreases progressively from ha-h-o-b or c. For the WN 3-5 stars there appears to be an opposite trend, the hydrogen richer stars being fainter.

The last two points may prove of interest with regard to the evolutionary sequences of WN stars.

3. The effect of hydrogen content

The aim of this section is to examine the effect of hydrogen content on T_* and to identify the group of WN stars that are entirely free of hydrogen. HKW have determined the temperatures T_* for most galactic WR stars by model fitting to the helium lines. They found (as confirmed in the previous section) that the ionisation subclasses are not clearly separated by either luminosity L or effective temperature T_*. However, they emphasised (as in Fig. 4) that the strong and weak line stars occupy different ranges of T_*. Fig. 6 shows the distribution of WN stars in the M_v vs. $\log T_*$ diagram, with the stars represented according to their broad, b, and hydrogen subclasses: ha, h and o. This is similar to Fig. 7 of HKW93 and to Fig. 4 of HKW95 but is confined to the stars with known M_v (including the improvements described in the previous section and Table 2) and includes the spectral separation of b, o, h (including (h)) and ha

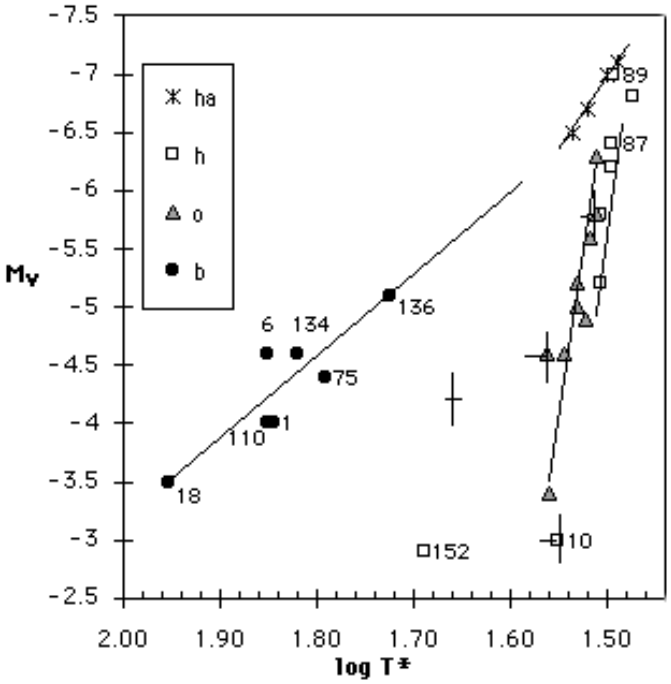

Fig. 6. The M_v vs. T_* diagram for WN stars with known distances. Symbols indicate the broad, b, and hydrogen subclasses: ha, h and o. M_v and T_* are from HKW, with corrections to M_v as described in Table 2 and Sect. 2.3. The error bars on single WR stars are ± 0.25 mag for M_v and ± 0.1 dex for $\log T_*$. WR stars in binaries have larger uncertainties in both co-ordinates and are indicated by small error bars up, down and to larger T_* (the direction of the T_* correction that has not been made).

stars. Binaries analysed by HKW have not been corrected for the companion, which will increase the derived T_*; however, those included in the diagram have luminosity ratios of O/WR less than 1 (see Table 2) and model fits by Howarth & Schmutz (1992) indicate that, so long as the WR is the brighter member of the pair, the resulting T_* is not greatly affected.

Fig. 6 shows some interesting features. As well as the clear separation of the broad line b-stars, we also see *a clear separation of the hydrogen subclasses: ha, h and o.* The ha-stars separate clearly (as in Fig. 5), with a flat slope at high luminosity. The difference between the h and o-stars is within the error bars for an individual point, however the average separation appears to be significant with the o-stars systematically hotter than the h-stars at the same M_v.

The h-star point on the ha line is WR 89 (WN 8h+abs) indicating that it is probably an ha star. WR 87 (WN 7+abs), which is in the same cluster with M_v nearly 1 mag fainter, falls with the other h-stars and the absorption lines are probably due to a companion.

On the basis of Fig. 6, we suggest that all narrow line stars (both o and h-stars) contain some hydrogen, with the difference that only the h-stars have sufficient hydrogen to be spectroscopically detectable; i.e. that the o-stars constitute the "missing" stars at low H/He in Fig. 2. We also suggest that the b-stars have *no* hydrogen; i.e. they represent the completely hydrogen

Table 2. Absolute magnitudes of WN stars other than given by HKW

WR	Spectrum	M_v(binary)	Ref.	Basis of correction	Ref.	L ratio O/WR	Δ m Individual	Δ m Adopted	M_v(WR)
6	WN4b	...	1	...	...	...	...	...	-4.6
10	WN5h(+ OB)	-4.2	2	EW 5411	1, 2	2 ?	1.2 ?	1.2	-3.0
46	WN3b pec (SB1)	-3.2	3	EW 5411	1, 3	3 ?	1.5?	1.5	-1.7
47	WN6o + O5V	-6.0	4	EW H9	4	0.5	0.4	0.7	-5.3
				EW 5411	1	1.4	1.0		
78	WN7h	...	5	...	...	...	...	...	-6.2
108	WN9ha	...	6	...	...	...	...	...	-7.1
127	WN3b + O9.5V	-4.8	4	EW H9, H11	4	3.3	1.6	1.6	-3.2
				EW 5411	1	3.0	1.5		
133	WN5o + O9I	-6.0	4, 5	EW emission	4	3.6	1.7	2.0	-4.0
					4	7.6	2.3		
				EW 5411	1, 2	11 ?	2.7?		
138	WN5o + B?	-5.3	2	Low absorp'n vis	4	0.4	0.4	0.4	-4.9
				EW 5411	1, 2	1.3?	0.9?		
139	WN5o + O6	-5.9	4	Eclipse photometry	4	4.4	1.8	1.8	-4.1
				EW 5411	1, 2	3 ?	1.5?		
141	WN5o + OB	-4.9	2	EW 5411	1, 2	0.3?	0.3?	0.3	-4.6
145	WN7o/CE + OB	-6.5	4	EW 5411	1	1.5	1.0	1.0	-5.5
153	WN6o/CE + O6I	-6.4	4	EW H9, H11	4	2.8	1.4	1.3	-5.1
				EW 5411	1	2.0	1.2		
155	WN6o + O9II/Ib	-6.3	7	Eclipse photometry	4	0.5	0.4	0.5	-5.8
				EW 4471 abs'n	4	0.6	0.5		
				EW 5411	1	5.0	1.9		
157	WN5o (+ B1 II)	-5.8	7, 5	EW 5411	1, 2	0.7?	0.6?	0.6	-5.2

References, M_v

1. Howarth & Schmutz (1995)
2. HKW93
3. Crowther et al. (1995b). The distance to WR 46 is based on interstellar lines and M_v is $\pm$ 1 mag.
4. van der Hucht et al. (1988)
5. Smith et al. (1994) revised the distance modulae of WR78 (NGC 6231), WR 133 (NGC 6871) and WR 157 (Ma50)
6. Crowther et al. (1995a). The distance to WR 108 is based on interstellar lines and M_v is $\pm$ 0.5 mag.
7. HKW95

References, basis of correction

1. SSM96 calibration of EW 5411 vs. FWHM 4686 and ionisation subclass.
2. Calibration for WN5 stars by SSM96 may overestimate the luminosity ratio, possibly overestimating the correction by 0.3 mag.
3. Lines from the companion of WR46 are not visible in the spectrum, making the correction to M_v rather doubtful. The star is not included in Figs. 5 & 6.
4. Smith & Maeder (1989) and references therein.

free phase of the WN stars. There are several reasons for this suggestion:

- The hydrogen-containing envelope is extended, as shown by stellar models. An increasing temperature as the hydrogen layer diminishes and a sudden jump to larger core temperature (below the optically thick wind) is expected when the last of the hydrogen is removed from the star.
- The closely correlated FWHM-EW relationships for each ionisation subclass (SSM96) have h-stars at the narrow-weak end proceeding through o to b-stars at the broad-strong end, suggesting a regular progression of decreasing hydrogen content.
- The simple linear relationship between T_* and M_v is suggestive of, and in the right sense (decreasing luminosity with increasing temperature) to match the Mass-L-T_* relationship required by the interiors models for these (relatively) simple stars. From the present data, the relationship for b-stars is:

$$M_v = 7 \log T_* - 38.2$$

and is used to derive the M_v of other b-stars, see Fig. 8 below. This relationship differs slightly from that originally suggested by HKW93 because of correction to the M_v of WR 136 (HKW95). All of HKW's derived values (used in later sections) have been corrected accordingly.

WR 149 (WN 5o) is included by HKW95 as a strong-line star because it has a thick atmosphere, a property that is

probably shared by all (or most) b-stars. (See the footnote in Sect. 2.2 regarding the stars WR 3 and 46.) WR 149 has a lower FWHM 4686 (20 Å) and larger EW 5411 (39 Å) than any other WN 5o star (see SSM96, Fig. 17). This is a combination that is exceptional in a population where these two parameters are extremely well correlated. While WR 149 fails the b-star criteria, we included it as an interesting object which appears closely related to the "fully developed" b-stars. Note that it falls in the intermediate region between b and non-b stars in Fig. 4.

Comment is given in the footnotes[2,3] on a few WN b stars that (may) have unusual features.

4. Are the WN b stars a one-parameter family?

A classification system aims to assign stars to categories within which the spectra are "very similar". The implicit hope is that the stars producing those spectra are also "very similar" - viz. in mass, composition, age and/or history. To the extent that this is true, the spectral type alone is able to indicate the age and stage of a star in its evolution.

Our hypothesis is that the WN b and only the WN b stars correspond to the hydrogen free phase of WN evolution. Evolutionary models predict that, in this phase, the previous history of the star is unimportant and that the mass is the critical parameter defining the properties of the star. We therefore examine the dominant spectral properties of the WN b to ascertain the degree to which this group may be regarded as a one-parameter family.

4.1. EW of HeII 5411 vs. log T_*

Fig. 6 (previous section) conforms to the primary prediction of the evolution models - the presence of a simple relationship between $\log T_*$ and M_v . In this section, we examine the relationships between log T_*, EW 5411, and FWHM 4686.

Fig. 7 shows the relationship between the EW of HeII 5411 and log T_*. Note that the points in this diagram are entirely independent of the M_v - T_* calibration. The relationship is extremely well defined; scatter around the line is much less than the observational uncertainty in log EW (± 0.07, for EW > 10 Å, according to SSM96). EW 5411 increases monotonically with T_* over subclasses WN 7b to WN 4b; the increase is more rapid in the WN 7 domain than at higher T_*.

T_* is derived from a model fit to HeII 5411 and HeI 5875. Schmutz et al. (1989, Fig. 6) show the contours of the two line strengths as functions of T_* and R_t, the transformed radius. The tight relationship in Fig. 7 reflects a restriction of the observed stars to a narrow band in the theoretically possible parameter space. The observed WN b stars follow the low-T_* "ridge" in the contours; i.e. the observed EW's of HeII 5411 are the *maximum allowed* by the models at any given value of T_*.

Fig. 8 shows the correspondingly good relationship between EW 5411 and M_v on the assumption that the log T_* - M_v relationship (Sect. 3) applies to all b-stars. The EW increases as the continuum brightness decreases to hotter sub-

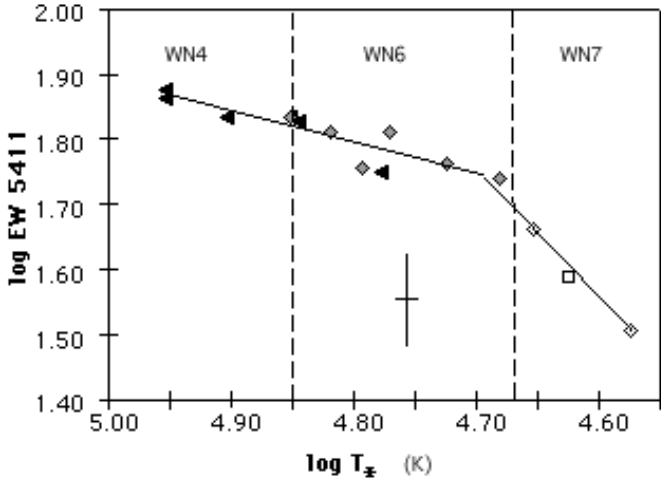

Fig. 7. Relationship of log EW 5411 to log T_* for WN b stars. The ionisation subclasses are indicated with the same symbols as in Fig. 8.

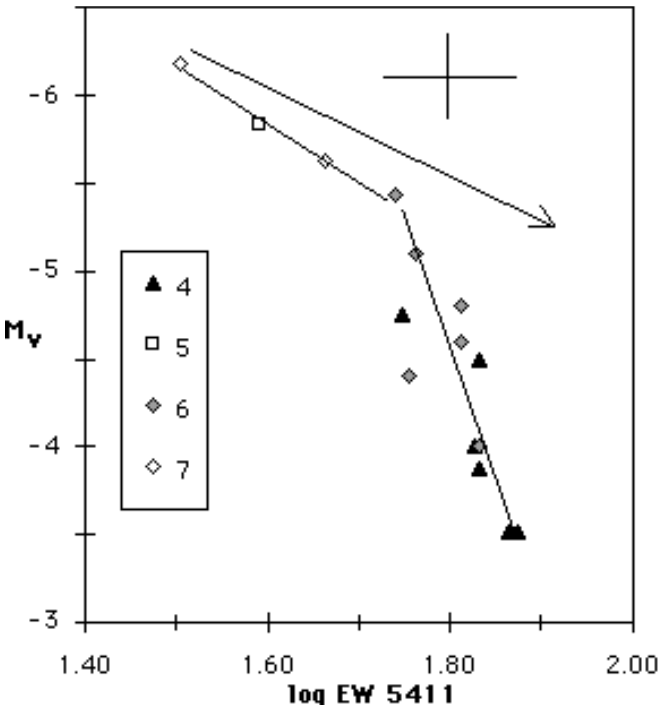

Fig. 8. Relationship between M_v and log EW 5411 for WN b stars on the assumption that the log T_* - M_v relationship (Sect. 3) applies to all b-stars. The ionisation subclasses are indicated for all points. The arrow indicates the slope of constant line-flux.

[2] WR 136 (WN 6b) is found by HKW93, Hamann et al. (1994) and Crowther & Smith (1996) to contain a small amount of hydrogen although the Pickering decrement is completely smooth. We note also that the T_* determinations by the two groups, both using pure helium models, differ by 0.2 dex. Thus, further analysis is needed of this controversial object.

[3] WR 36 and 110 were (with much discussion) assigned a classification of WN 5-6 by SSM96. For simplicity, we relegate them to WN 6, noting that the subclass WN 5 is distinguished by its nitrogen spectrum rather than by the HeII/I ratio, which overlaps WN 4 and WN 6.

classes. For the WN 7b stars, the rate of increase is only slightly lower than for constant line-flux (indicated by the arrow in Fig. 8); i.e. these stars have nearly constant HeII 5411 flux implying that the "size" (integral n_e^2) of the atmosphere is nearly constant while the continuum brightness of hotter stars is lower. In the WN 6 to 4 domain, the rate of increase of EW 5411 with decreasing M_v is much lower than for constant flux. That is, the flux from the atmosphere is *de*creasing steeply as we move to higher T_* but the brightness of the continuum (the star) is decreasing even more steeply. This relationship is potentially useful since it allows us, in principle, to estimate the M_v of a WN b star from the EW 5411. Its usefulness, in practice, is limited by the typical uncertainty of ± 0.07 in log EW. The lines in Fig. 8 are:

M_v = 3.3 log EW 5411 - 11.1, for log EW < 1.74

M_v = 15 log EW 5411 - 31.4, for $1.74 <$ log EW < 1.95

On the basis of their behaviour in M_V, T_* and EW 5411, the b-stars appear to be a one-parameter family in which radius R_*, luminosity L, and line flux decrease as effective temperature T_* and EW 5411 increase.

4.2. FWHM of HeII 4686 vs. log T_*

In contrast to EW 5411, the behaviour of FWHM 4686 (i.e. the terminal velocity, see Fig. 1) is complex.

SSM96 have shown that, within an ionisation subclass, there is a very tight correlation between EW 5411 (i.e. T_*, see Fig. 7) and FWHM 4686 (terminal velocity, see Fig. 1). Fig. 9 plots FWHM 4686 vs. log T_* with the ionisation subclasses distinguished by symbols. Because of the very tight EW 5411 - T_* relationship for WN b stars, Fig. 9 corresponds to the EW 5411 vs. FWHM 4686 diagram of SSM96. In marked contrast to the tight correlation of EW 5411 and T_*, the spread of FWHM 4686 at constant T_* is very large and the error bars are very small.

The spread of FWHM 4686 at a given value of log T_* indicates that a second parameter must be important in defining the velocity structure of the wind.

A clue to an explanation of the spread of v_∞ comes from a comparison of Figs. 4 and 9. The stars in Fig. 4 that have significantly low HeII/I for their value of T_*, namely WR 36, 75 and 110, are the same stars that in Fig. 9 have the largest FWHM, 45 Å or above. The second parameter involved appears to be the extent/optical thickness of the atmosphere.

Fig. 10 shows the mass loss rate, $\dot{M}$, and the surface mass flux as functions of T_* with the lines drawn through the stars of lowest FWHM 4686 as in Fig. 9. The same three stars WR 36, 75 and 110 fall the farthest above the line in both mass loss parameters. We also note that the WN 5o star (WR 149) which has been included as a curiosity (see Sect. 3.1) is distinguished by low values of both mass loss parameters, consistent with our suspicion that it is not yet a full member of the "b" subclass but is in the process of loosing the last of its hydrogen shell and increasing its mass loss rate.

The behaviour of FWHM 4686, EW 5411, HeII/I and the mass loss parameters as functions of T_* suggests the following:

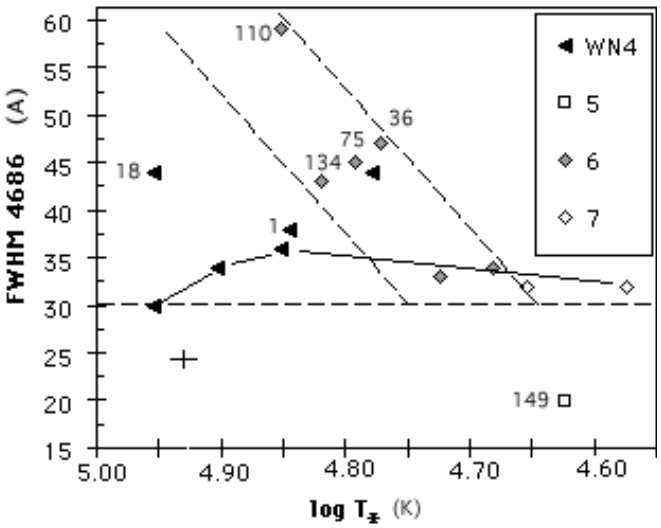

Fig. 9. Relationship between FWHM 4686 and log T_* with the ionisation subclasses distinguished by symbols. The sloping dashed lines give near separation of the ionisation subclasses, corresponding to the EW-FWHM correlations found by SSM96 within each subclass. The dashed line at FWHM = 30 Å indicates the lower limit for b-star classification. The solid line passes through (to observational accuracy) the stars of lowest FWHM. Its significance is discussed below in relation to later diagrams.

- The tight correlation between EW 5411 and T_* results from a Strömgren sphere, ionisation-limitation of the HeII region of the atmosphere. T_* is essentially a Zanstra temperature.
- The extent of the HeI region (beyond the HeII zone) is controlled by the surface mass flux.
- At a given T_*, both $\dot{M}$ and surface mass flux have a significant range. Those stars with higher surface mass flux have a larger HeI region (at constant T_* and EW 5411) resulting in a lower ratio of HeII/I and an increased optical thickness of the atmosphere.
- Opposing effects of increasing T_* (which increases EW HeII 5411 and increases the HeII/I ratio) and increasing extent of the HeI region (which increases EW HeI 5875 and decreases the HeII/I ratio) leads to the scatter and to the sloped subclass divisions in the HeII/I - T_* plane (Fig. 4).
- *Increasing opacity of the atmosphere correlates with increasing width of HeII 4686* (Fig. 9).

The critical question then is: Why, at a constant mass and T_*, does the surface mass flux and, therefore, the atmospheric opacity vary? This will be addressed in Sect. 6 after we have further discussed the evolutionary models.

The separation of the b-stars from the o and h-stars (Fig. 4) may be understood in the same fashion. The later stars have larger radii and lower T_* due to the presence, in both subclasses, of an extended hydrogen envelope. However, the o and h-stars do not have optically thick atmospheres and, therefore, at a given value of T_*, have a higher ratio of HeII/I.

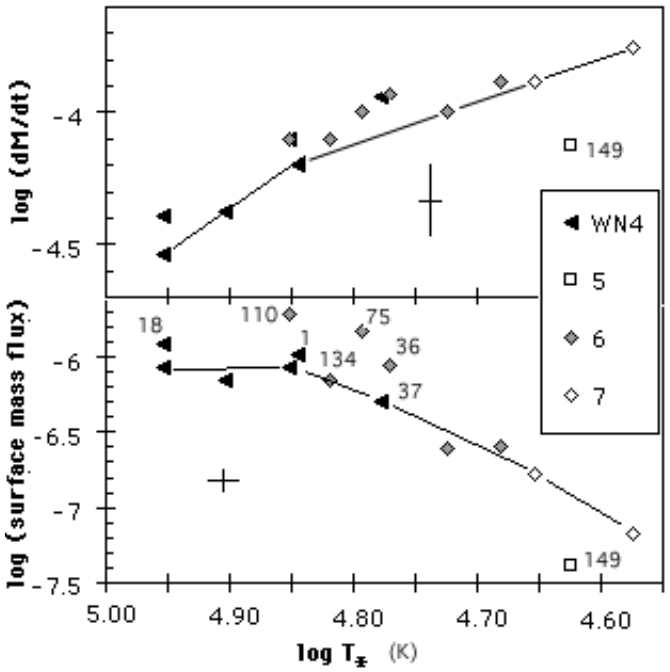

Fig. 10. Relationships of $\dot{M}$, and surface mass flux to T_*. The points are from HKW95 (corrected for the change in the M_v - T_* relationship). The lines pass through the stars of lowest FWHM 4686, as in Fig. 9. The stars with high $\dot{M}$ and surface mass flux for their value of T_* also have low HeII/I (Fig. 4) and large FWHM 4686 (Fig. 9) i.e. large terminal velocity.

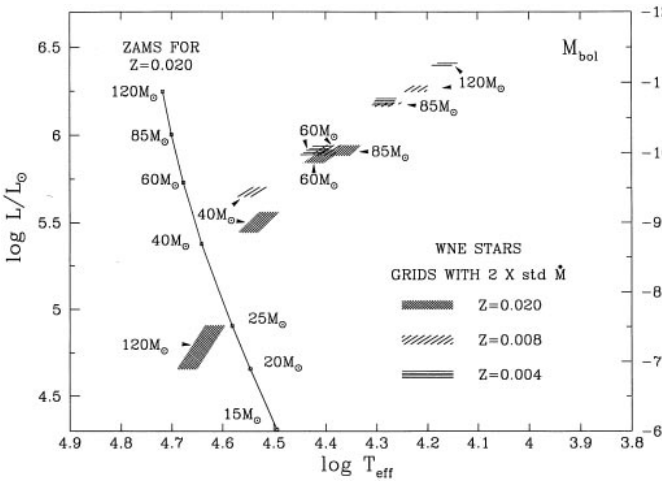

Fig. 11. Location in the temperature-luminosity diagram of the stellar models that correspond to WN stars free of hydrogen. The region occupied by the H-free WN phase has been, up to now, called the WNE band (cf. Maeder & Meynet 1994). We now designate it the WN b band.

5. Comparison of atmosphere and evolutionary models of WN b stars

Our aims in this section are: to compare the predictions of the evolutionary models with the observed stars (interpreted by atmosphere models); to highlight the existing problems with such a comparison; and to indicate directions in which improvement may be most readily forthcoming.

Fig. 11 (cf. Maeder & Meynet 1994) shows the overall prediction of evolutionary models: WN stars, once free of their hydrogen envelope, lie along a band in the temperature-luminosity diagram. This band has been previously designated WNE by model builders. However, since some WNE (meaning WN 2-6 stars) still have hydrogen, this band (if our hypothesis is correct) should be called the WN b band or phase. When a star (of sufficient mass) looses its last hydrogen shell, it settles onto the WN b band. Then, as a result of continued mass loss, the luminosity decreases and the temperature increases, so that the star moves *along* the band. Its position on the WN b band depends only on its mass (see also Sect. 6). When the products of He-burning appear at the surface, the star leaves the WN b band and settles onto the WC band, which is slightly cooler.

Placing observed WR stars into the theoretical HR diagram (log T_* vs. log L) presents several problems of which the most acute are that the definition of T_* is ambiguous and that the B.C. determined from the atmospheric models appear to be underestimated.

We compare the results of atmospheric models for WN b stars (HKW95) to evolutionary Co-star models by Schaerer (1995; 1996) and Schaerer et al. (1996ab). Parameters available for comparison are, in principle: luminosity L; effective temperature T; and radius R. However, these three are redundant since they are uniquely related via the black body relationship. In WR stars, the definition and determination of T and R are complicated by the presence of the expanding atmospheres. This complication is handled differently by atmospheric and evolutionary models.

Atmosphere models fit the strength (and profiles in a "tailored analysis") of the helium lines to determine T_* at τ = 10 or 20. The luminosity L comes from the observed or assumed M_v plus the B.C. (from the models) and the radius R follows from the black body relationship.

Evolutionary models (mostly concerned with the interiors) add a parameterised atmosphere to the hydrostatic interior model. (The atmosphere model is similar to that used by the atmosphere calculations but assumes a dependence of the wind parameters, $\dot{M}$ and v_∞, on parameters defined by the interior model.) The luminosity L comes from the interior model, $R(\tau)$ comes from the assumed velocity law and the superposed model atmosphere and T follows from the black body relationship.

It has been known for some time (e.g. Howarth & Schmutz 1992) that, for stars of known mass and M_v , the luminosities derived using B.C.'s from atmosphere models fall short of those required by the interior models. Since there appears to be no uncertainty in the mass-luminosity relationship for WR stars, the conclusion must be that the B.C. are underestimated by the pure helium atmosphere models. Various explanations have been suggested. Heger & Langer (1997) suggest that some of the discrepancy may be due to the mechanical energy that leaves the star in the wind. Crowther et al. (1995) found that He-N models for two weak line stars yield higher values of T_* than do H-He models; however, Hamann et al. (1994) find no

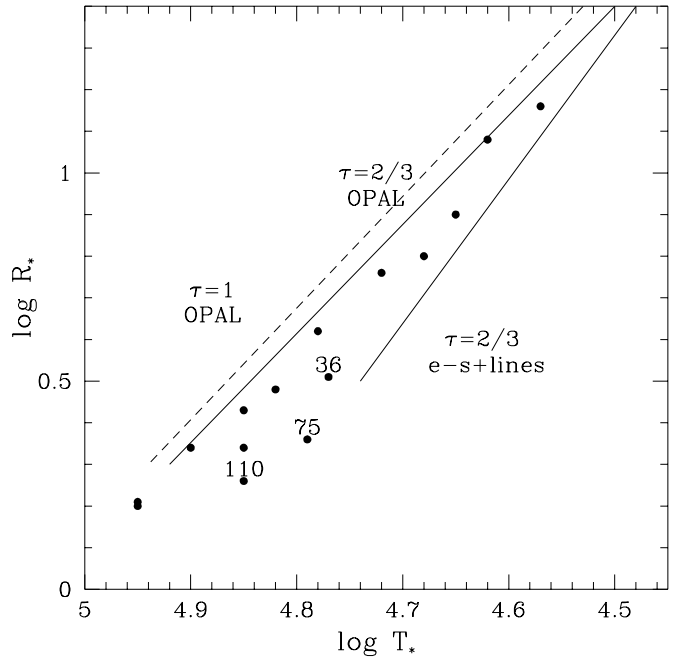

Fig. 12. The WN b stars in the $\log R_*$ vs. $\log T_*$ diagram. Points are data from HKW95, with T_* determined at $\tau = 10 - 20$ (and with correction for the improved M_v - T_* relationship). Solid lines represent Schaerer's models (1995, plus line opacities treated with a force multiplier. The dashed line represents Schaerer's models for $\tau = 1$ with OPAL opacities.

significant difference. Schmutz (1996) shows that inclusion of photon losses and their effect on the ionisation balance lead to higher values of T_*.

Bearing in mind that the "evolutionary" L, and therefore T_*, may be overestimated (if mechanical energy is significant) and the "atmosphere" L, and therefore R_*, are probably underestimated, we now compare the temperature-radius diagrams that result from HKW95's pure helium atmosphere models applied to individual stars with predictions of the Co-star models by Schaerer (loc. cit.). We choose the R_*-T_* diagram rather than the L-T_* diagram since it appears to better illustrate the problem we wish to highlight.

Fig. 12 shows the $\log R_*$ vs. $\log T_*$ diagram for atmospheric models of WN b stars from HKW95; R_* has been modified to allow for the improved M_v - T_* relationship. The data shows a scatter of about ± 0.1 in $\log R_*$, which is a reasonable "observational uncertainty". The lines are from Schaerer's models for various optical depths and opacities: $\tau = 2/3$ and 1.0 with OPAL opacities (Iglesias et al. 1992, Iglesias & Rogers 1993) and $\tau = 2/3$ with opacities (as described by Schaller et al., 1992) based on electron scattering and a force multiplier to allow for the contribution of spectral lines (cf. Kudritzki et al. 1989, Schmutz 1991).

The atmosphere models lie neatly between the two $\tau = 2/3$ lines (solid lines) of the evolutionary models. The underestimate of T_* and R_* by the atmosphere models (see above) would bring the points into relatively good agreement with the (solid) line representing the OPAL opacity models for $\tau = 2/3$. However, the apparent agreement is illusory since T_* of HKW95 were derived at $\tau = 10 - 20$ not at $\tau = 2/3$. HKW's models at $\tau = 2/3$ give values of $\log T$ near 4.5 for all stars. Conversely, Schaerer's models at $\tau = 10$ or 20 give values of log T near 5.0, or 5.1, respectively, for all stars.

Thus, the primary result of our comparison of atmospheric to interior models is a large difference between the temperatures and/or the optical depths derived by HKW and by Schaerer (loc. cit.).

The disagreement appears to hinge on the connection between R and τ which is, in principle, defined by the assumed velocity law. Different choices of the exponent beta in the wind velocity law (HKW use $\beta = 1$; Schaerer uses beta = 2.1) will (according to Schaerer) give a difference of 0.23 dex in τ which is in the right direction but insufficient to account for the disagreement between the two sets of models. However, since the velocity law probably does not correspond to reality, the result may be acute sensitivity to boundary conditions such as the core radius.

We conclude that there is a qualitative correspondence between the evolutionary models and the observed stars interpreted by atmosphere models; in particular that the WN b stars appear to follow a simple relationship of their basic stellar properties indicating a one-parameter family. However, there appear to be systematic errors that make $\tau = 2/3$ in Schaerer's treatment occur at approximately the same radius as $\tau = 10 - 20$, in HKW's treatment of the atmospheres.

6. Terminal velocities: Stellar parameters affecting the wind

In Sect. 4.2, we highlighted the spread in observed FWHM 4686, HeII/I and mass loss parameters at a given value of T_*. This spread indicates that WN b stars which are similar in T_*, R_* and L, parameters that are simple functions of the mass (see Sect. 7), may still have a significant range of wind parameters (cf. Heger & Langer 1997 who come to the same conclusion for different reasons). The wind parameters highlighted in Sect. 4.2 as critical were the surface mass flux and, thence, the atmospheric opacity.

The critical question then is: Why and how, at a constant mass and T_*, does the surface mass flux and, therefore, the atmospheric opacity vary? What is the second parameter, after mass of the star, that affects the wind?

In this section, we consider four stellar properties which might be, for WN b stars, such a second parameter: 1) the mass fraction of the convective core; 2) the fraction X_{C+O} of carbon and oxygen in the convective core; 3) the mass fraction f_{CO} occupied by the region with X_{C+O} greater than some value, e.g. 0.05; 4) the rotation rate of the star.

1. The mass fractions of the convective cores in WN b stars are predicted by evolutionary models (cf. Meynet et al. 1994) to be more or less in a one-to-one relationship with the actual mass of the star, independent of the initial metallicity and previous history. The physical reason for this one-to-one

relationship is that WN b stars of the same mass have about the same temperature gradient and therefore reach convective instability at the same depth. Thus, the mass fraction of the convective core cannot introduce a second parameter.

2. The fraction X_{C+O} of carbon and oxygen in the convective core can be very different in WN b stars with the same mass. The reason is that a higher mass loss rate during the previous evolutionary phases, due to higher initial mass or higher Z, leads to a lower mass at any subsequent stage of central nuclear evolution. Conversely, for a given present mass, a WN b star originating from a higher initial mass or higher Z will have a lower central X_{C+O}. This is the effect that, in the WC phase, determines the surface abundance and hence the subclass of the WC star (cf. Smith & Maeder, 1991).
   Central X_{C+O} may influence the mass flux through pulsational instability. The significance of pulsational instability to the WR phase was suspected early (see review by Smith, 1968b) and has gained support because the instability to core pulsation is predicted to appear at the WR phase of evolution (Maeder 1985). Recent pulsation models for WR stars (cf. Schaller 1991) indicate that pulsational instability increases with the central X_{C+O} content and with the mass fraction f_{CO} of the CO rich region. This relationship was established qualitatively for homogeneous stellar models (cf. Ledoux 1951), for which the maximum mass M_{max} for vibrational stability obeys the relationship: $\mu^2 M_{max} \simeq$ constant, where μ is the mean molecular weight. Thus, if pulsational instability plays a role in mass loss, we would have a simple physical connection between the central composition and the mass flux.

3. The mass fraction f_{CO} increases significantly during the WN b phase. At the entry to this phase, f_{CO} is close to the mass fraction of the convective core, typically about 0.6; at the end of the WN b phase, the star enters the WC phase and f_{CO} is equal to one. The central X_{C+O} and the value of f_{CO} are, of course, increasing together and both lead to an increase of the internal mean molecular weight and of the pulsational instability. As in 2), above, this could lead to an increase in the mass flux.
   In summary, stellar properties 2) and 3) suggest that the second parameter that affects the speed and extent of WN b star winds could be the internal mean molecular weight, μ, increasing the mass loss rate and v_∞ through the effects of pulsation.

4. Stellar rotation has at least two main effects. It can induce internal mixing, thus affecting the internal structure and evolution. The main result of mixing is a change in the average μ and its distribution and, in this respect, is the same as properties 2) and 3) above. However, rotation may also greatly affect the geometric and density structure of the stellar wind, thus directly modifying the widths of the emission lines. At present, nothing is known about the rotational velocity of WR stars.

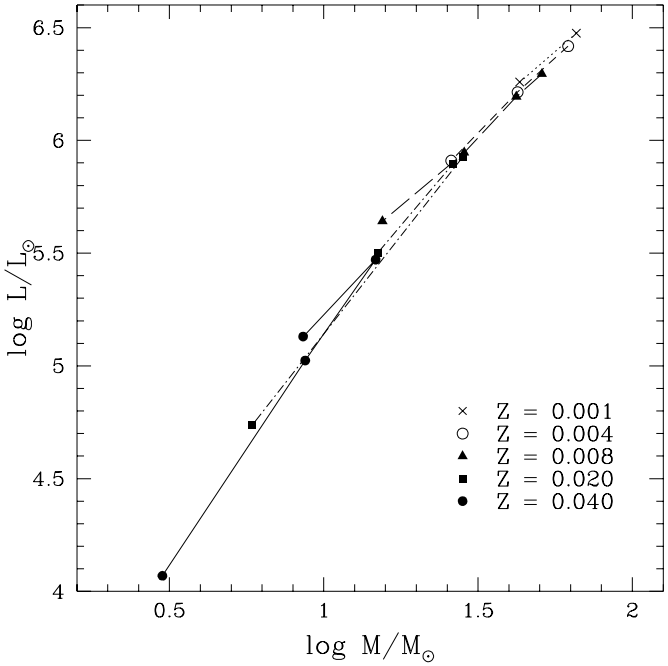

Fig. 13. The mass-luminosity relation for WN-stars without hydrogen (from models by Meynet et al. 1994).

In summary, the second parameter affecting the wind properties, v_∞ and mass flux, of WN b stars appears likely to be either (or both of) the internal μ or the rotation rate.

7. Conclusions

The correlations between various parameters of the WN b stars supports the idea that they are an essentially one-parameter family. Specifically, the WN b stars follow, within the observational uncertainty, one-to-one relationships in the following plots:

- M_v vs. $\log T_*$ (Fig. 6);
- $\log$ EW 5411 vs. $\log T_*$ (Fig. 7);
- $\log$ EW 5411 vs. M_v (Fig. 8);
- $\log R_*$ vs. $\log T_*$ (Fig. 12).

The primary parameter defining the properties of a WN b stars is certainly its present mass. Fig. 13 shows the mass-luminosity relationship for WN stars without hydrogen from models by Meynet et al. (1994). Models of different initial metallicities obey the same, well defined relationship. The mass-luminosity relationship is independent of the local Z and of the previous history of the star. This will eventually allow the assignment of masses corresponding to the other tightly correlated parameters: T_*, R_*, M_v and EW 5411.

The actual mass of a WN b star is also related to its initial stellar mass. Fig. 14 shows the relationship for different

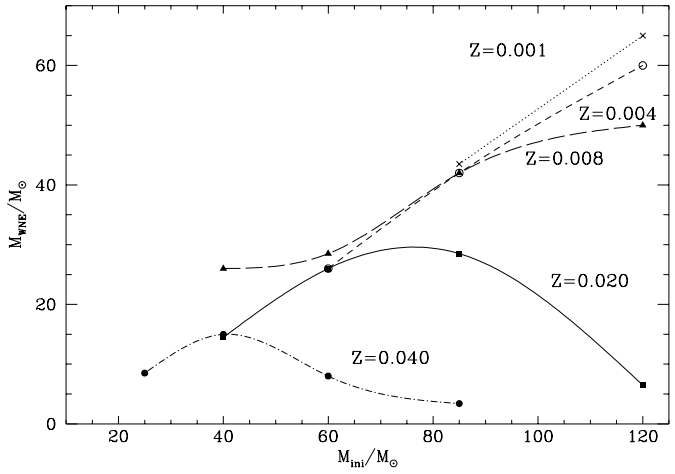

Fig. 14. The relation between the actual mass of WN-stars without hydrogen and their initial masses for various metallicities Z (from models by Meynet et al. 1994).

metallicities from the models by Meynet et al. (1994). The relationship is very sensitive to Z and, for $Z \geq 0.02$, it is double valued; i.e. a given WN b star mass can result from two different initial stellar masses, even at the same Z. Thus it does not appear possible to assign an initial mass to a WN b star on the basis of its present mass or other properties.

While most parameters of WN b stars are well correlated with each other, the line width, represented by FWHM 4686, is an exception (Fig. 9). This suggests the presence of a second parameter that affects the mass flux and the terminal velocity of the optically thick wind. The discussion in the previous section suggests that this second parameter may be either (or a combination of) internal mean molecular weight or rotation rate.

References

Beals C.S., 1938, Trans IAU 6, 248
Crowther P.A., Hillier D.J., Smith L.J., 1995a, A&A 293, 172
Crowther P.A., Smith L.J., Hillier D.J., 1995b, A&A 302, 457
Crowther P.A., Smith L.J., 1996, A&A 305, 541
Eenens P.R.J., Williams P.M., 1994, MNRAS 269, 1082
Hamann W.-R., Koesterke L., Wessolowski U., 1993, A&A 274, 397 (HKW93)
Hamann W.-R., Wessolowski U., Koesterke L., 1994, A&A 281, 184
Hamann W.-R., Koesterke L., Wessolowski U., 1995, A&A 299, 151 (HKW95)
Heger A., Langer N., 1997, A&A in press
Hiltner W.A., and Schild R.E., 1966, ApJ 143, 770
Howarth I.D., Schmutz W., 1992, A&A 261, 503
Iglesias C.A., Rogers F.J., Wilson B.G., 1992, ApJ 397, 717
Iglesias C.A., Rogers F.J., 1993, ApJ 412, 752
Kudritzki R.P., Pauldrach A., Puls J., Abbott D.C., 1989, A&A 219, 205
Langer N., 1989a, A&A 210, 93
Langer N., 1989b, A&A 220, 135
Ledoux P., 1951, ApJ 114, 373
Lundström I., Stenholm B., 1984, A&AS 58, 163
Maeder A. 1983, A&A 120, 113
Maeder A., 1985, A&A 147, 300
Maeder A., and Meynet G., 1994, A&A 287, 803
Meynet G., Maeder A., Schaller G., Schaerer D., Charbonnel C., 1994, A&AS 103, 97
Morris P.W., Brownsberger K.R., Conti P.S., Massey P., Vacca W.D., 1993, ApJ 412, 324
Prinja R.K., Barlow M.J., Howarth I.D., 1990. ApJ 361, 607
Schaerer D., 1995, PhD thesis, Geneva Observatory
Schaerer D., 1996, A&A 309, 129
Schaerer D., de Koter A., Schmutz W., Maeder A., 1996a A&A 310, 837
Schaerer D., de Koter A., Schmutz W., Maeder A., 1996b A&A 312, 475
Schaerer D., Maeder A. 1992, A&A 263, 129
Schaerer D., Meynet G., Maeder A., Schaller G., 1992, A&AS 98, 523
Schaller G., Schaerer D., Meynet G., Maeder A., 1992, A&AS 96, 269
Schaller G., 1991, PhD thesis, Geneva Observatory
Schmutz W., 1991 NATO ASI Series C 341, p.191
Schmutz W., Vacca, W.D., 1991 A&AS 89, 259
Schmutz W., 1996 in "Wolf-Rayet stars in the framework of stellar evolution", Proc. 33rd Liège Coll., Ed. J.M. Vreux et al., p. 553
Schmutz W., Hamann W.-R., Wessolowski U., 1989, A&A 210, 236
Smith L.F., 1968a, MNRAS 138, 109
Smith L.F., 1968b, in "Wolf-Rayet Stars", National Bureau of Standards Special Publication 307, eds. K.B. Gebbie & R.N. Thomas, US Gov Printing Office. pp 50 & 151 (the discussion)
Smith L.F., Maeder A., 1989, A&A 211, 71
Smith L.F., Maeder A., 1991, A&A 241, 77 (Paper I)
Smith L.F., Meynet G., Mermilliod J.-C. 1994, A&A 287, 835
Smith L.F., Shara M.M., Moffat A.F.J., 1996, MNRAS 281, 163 (SSM96)
Vacca W.D., Torres-Dodgen A.V., 1990, ApJS 73, 685
van der Hucht K.A., Conti P.S., Lundström I., Stenholm B., 1981, Space Sci.Rev. 28, 227